



HAL
open science

An Integrative Approach to Decipher the Chemical Antagonism between the Competing Endophytes *Paraconiothyrium variable* and *Bacillus subtilis*

Marine Vallet, Quentin P. Vanbellinghen, Tingting Fu, Jean-Pierre Le Caer, Serge Della-Negra, David Touboul, Katherine R. Duncan, Bastien Nay, Alain Brunelle, Soizic Prado

► **To cite this version:**

Marine Vallet, Quentin P. Vanbellinghen, Tingting Fu, Jean-Pierre Le Caer, Serge Della-Negra, et al.. An Integrative Approach to Decipher the Chemical Antagonism between the Competing Endophytes *Paraconiothyrium variable* and *Bacillus subtilis*. *Journal of Natural Products*, 2017, 80 (11), pp.2863-2873. 10.1021/acs.jnatprod.6b01185 . hal-01998984

HAL Id: hal-01998984

<https://hal.science/hal-01998984v1>

Submitted on 13 Mar 2024

HAL is a multi-disciplinary open access archive for the deposit and dissemination of scientific research documents, whether they are published or not. The documents may come from teaching and research institutions in France or abroad, or from public or private research centers.

L'archive ouverte pluridisciplinaire **HAL**, est destinée au dépôt et à la diffusion de documents scientifiques de niveau recherche, publiés ou non, émanant des établissements d'enseignement et de recherche français ou étrangers, des laboratoires publics ou privés.

An integrative approach to decipher the chemical
communication between the competing endophytes

Paraconiothyrium variable and *Bacillus subtilis*

Marine Vallet,^{†,‡} Quentin P. Vanbellingen,[‡] Tingting Fu,[‡] Jean-Pierre Le Caer,[‡] Serge Della-
Negra,[‡] David Touboul,[‡] Katherine R. Duncan,[§] Bastien Nay,[†] Alain Brunelle,[‡] Soizic Prado[†]

[†]Unité Molécules de Communication et Adaptation des Micro-organismes (UMR 7245),
Sorbonne Université, Muséum national d'Histoire naturelle, CNRS, CP 54, 57 rue Cuvier, 75005
Paris, France

[‡]Institut de Chimie des Substances Naturelles, CNRS UPR2301, Univ. Paris-Sud, Université
Paris-Saclay, Avenue de la Terrasse, 91198 Gif-sur-Yvette, France

[‡]Institut de Physique Nucléaire, UMR8608, IN2P3-CNRS, Université Paris-Sud, Université
Paris-Saclay, 91406, Orsay, France

[§] Strathclyde Institute of Pharmacy and Biomedical Sciences, HW608, University of Strathclyde,
161 Cathedral Street, Glasgow, UK.

KEYWORDS: endophytes, mass spectrometry imaging, microbial competition, chemical communication, molecular networking, surfactin, tetronic acid.

ABSTRACT: To interact with one another and respond to environmental cues, microorganisms communicate with their own chemical languages using a wide range of extracellular signals and cellular responses. However, identification of these signaling molecules remains elusive, as does the assessment of their biological significance. Endophytes are microorganisms (both bacteria and fungi) that live within plants, most of them without causing any symptom of disease. They have drawn a growing interest worldwide especially for their enormous taxonomic diversity but also for their capability to biosynthesize secondary metabolites. Moreover, the precise role of such endomicrobiota within the host-plant as the ecological significance of their metabolites remains underexplored.

In this context, we have undertaken an integrative approach dealing with traditional natural products chemistry, molecular networking and mass spectrometry imaging to decipher the molecular dialogue between the fungus *Paraconiothyrium variabile* and the bacterium *Bacillus subtilis* which have been both isolated as endophytes from the conifer *Cephalotaxus harringtonia* and are characterized by a strong and mutual antibiosis. From this study, we highlight that bacterial surfactins and a fungal tetronic acid are involved in such competition and that the fungus is able to hydrolyse surfactins to fight against the bacterial partner.

INTRODUCTION.

Communication is understood as a process by which information is exchanged between living individuals through a common system of symbols, signs, tones or behaviour. In bacteria, lower eukaryotes, fungi and plants, the modes of intra and interspecies communication appear to be mainly of chemical nature.¹ Thus, to interact with one another and respond to environmental cues, microorganisms communicate with their own chemical languages using a wide range of extracellular signals and cellular responses.² Nevertheless, in several cases, identification of these signaling molecules remains elusive, as does the assessment of their biological significance.

Endophytes are microorganisms that live within plants, most of them without causing any symptom of disease.³ They have drawn a growing interest worldwide not only for their enormous biological diversity but also for their capability to biosynthesize secondary metabolites.^{4,5} Nevertheless the precise role of such endomicrobiota within the host-plant as well as the ecological role of their metabolites remains underexplored.

In a previous study, we showcased the cultivable fungal diversity present in the leaves of *Cephalotaxus harringtonia* (Knight ex J. Forbes) K. Koch,⁶ an Asian medicinal plant rich in cytotoxic compounds, whose phytochemical content has been well studied in our laboratory.⁷⁻⁹ More than 640 isolates and bacterial isolates were identified by ITS rDNA sequencing and 16S rDNA, respectively.⁶ Among them, the fungus *Paraconiothyrium variable* (LCP5644) and the bacterium *Bacillus subtilis* (9E1a) were isolated and exhibited a strong and mutual antibiosis. The fungus *P. variable* is now biologically well-characterized in our laboratory and its chemistry has not been explored until now. According to our previous work this fungus showed interesting biological or chemical properties, being antagonistic against a phytopathogen,¹⁰ using plant

metabolites for its own benefit¹¹ or showing bioconversion potential for synthetic purposes.¹² Interestingly, *P. variable* has also been recently isolated from *Taxus baccata* and was shown to be paclitaxel producer.¹³ On the other hand, the position of *B. subtilis* as an endophyte is still debated even though Firmicutes (the clade to which *B. subtilis* belongs) have been commonly described as endophytic bacteria.¹⁴ In any case, *B. subtilis* constitutes a good model for a bacterium closely associated with plants especially since its genome has been fully sequenced.¹⁵

It has been suggested that the secondary metabolites responsible for antagonistic effects may only be produced in response to interactions with other stressing microorganisms (inducible metabolites) unlike constitutive metabolites. Accordingly, many recent studies provided compelling evidence that microbial interactions can play major roles in the onset of metabolite production⁴ and that the growth of different microorganisms together forces direct interactions that may induce the production of compounds not previously observed when the strains are grown independently.¹⁶⁻¹⁹

As a result, the characterization of the metabolites produced in a microbial consortium is more relevant if metabolites are detected and isolated in co-cultured system and in our case in the zone of inhibition. However, only restricted amounts of material can be isolated from solid cultures, therefore very sensitive analytical techniques are required. With the advent of new investigative tools dealing with microbial competition, this should permit better characterization of the molecular interaction in a microbial system.

Among those, molecular networking compares metabolite profiles based on parent ion fragmentations. This method has been used to chemically dereplicate complex crude extracts and to prioritize metabolites for structure elucidation.²⁰⁻²² Novel bioactive compounds have been thus discovered using molecular networking approach such as vitroprocines A-J isolated from a marine

Vibrio sp.,²³ colombamides produced by marine cyanobacteria²⁴ or the quinomycin-type depsipeptide retimycin A isolated from the obligate marine bacteria *Salinispora*.²⁵ Recently, molecular networking has been also successfully applied to determine the quantitative change of microcystin production in the course of cyanobacterial co-culturing experiments.²⁶

In addition, the advances in instrumentation such as time-of-flight (TOF) mass analysers and ionization methods, such as matrix-assisted laser desorption/ionisation (MALDI), enhanced the sensitivity of mass spectrometry techniques and allowed metabolite events associated with microbial competition to be addressed. Indeed, the emerging technology of Mass Spectrometry Imaging (MSI) is now capable of recording the spatial distribution of metabolites secreted by microorganisms directly on agar medium and has been successfully applied to small molecules such as natural products.^{27,28} Two main MSI techniques: MALDI-TOF and TOF-SIMS (Secondary Ion Mass Spectrometry), allow detection of different mass ranges and different classes of compounds. The first one is the most widely used and was successfully applied using microbial MSI^{25,29-31} to monitor the surfactin production of *Bacillus* spp.^{32,33} TOF-SIMS imaging has also been used to localize the surfactins produced during *Bacillus* sp. swarming transferred onto a silicon wafer.²⁸

In this study molecular networking, MALDI-TOF and TOF-SIMS have been used to decipher and map the chemistry of the microbial competition between the endophytes *P. variable* and *B. subtilis* on agar. A new method was designed to optimize the sample preparation allowing bacterial surfactins and their hydrolyzed analogues to be detected independently using two MSI methods. The response of *P. variable* to the bacterial challenge was assessed. The fungus was found to hydrolyze the surfactant lipopeptides and to produce antimicrobial tetronic acids against bacteria. This work therefore provides new insights in the comprehension of the chemical

mediation involved in the course of interspecies interaction within the endophytic microbiota of a host-plant.

RESULTS AND DISCUSSION.

Interspecific microbial competition of endophytes

Among the endophytic microbial strains obtained from the leaf of the conifer *C. harringtonia*, *P. variable* LCP5644 and *B. subtilis* 9E1a showed a strong and unique antagonism during their isolation, which was never observed between other partners of the plant-microbiota (Figure 1). This antagonism was persistent as no covering was observed after 60 days of culture (data not shown) and is characterized by the inhibition of the aerial hyphae development of the fungus as represented in Figures 1B and 1D. This effect is referred to as a balding effect and has already been described in the course of the interaction between *B. subtilis* and *Streptomyces coelicolor*.³³ As represented in Figures 1A and 1B, the bacterium is also affected by the presence of the fungus, as no bacterial growth is visible in front of *P. variable*. Furthermore, no competition was detected when the microorganisms were grown in a divided Petri dish, suggesting the involvement of a diffusible chemical rather than volatile organic compounds production (data not shown).

The numbers of studies reporting bacterium-fungus interactions have increased during the last few years, and some secondary metabolites, which orchestrate the associations, have been identified. Among the different categories of bacterial-fungal molecular interactions (*e.g.*, signaling-based interactions, interactions *via* modulation of the physicochemical environment, chemotaxis, interactions *via* cooperative metabolism or *via* protein secretion and gene transfer), the best-known and most extensively studied is antibiosis.³⁴ Indeed, this kind of interaction involves a chemical warfare mediated by the production of deleterious diffusible molecules from

one partner to the other. With the aim to decipher the compound-based signals involved in the competition between the endophytes, we undertook the study of the metabolites specifically produced in the competition zone by using molecular networking and comparing them with the metabolites produced independently by each microbial partner.

Molecular network analysis of the metabolites produced in the course of the competition

The molecular network shows the comparative metabolomics of 12 crude extracts including extracts from the bacterial, the fungal and the competition zones, respectively (all in triplicate, $n=3$), in addition to one extract of the culture media (control, also in triplicate, $n=3$). Analysis of MS/MS data led to the identification of 2672 precursor ions which were visualised as nodes in the molecular networking and are connected by 3726 edges with a cosine score varying from 0.7 to 1 (a cosine score of 1 corresponds to two identical MS/MS spectra) (Figure 2).

The molecular network was seeded with known compounds from the Global Natural Products Social (GNPS) molecular networking standards library, in which one molecular family (groups of related precursor ions) encompassed standards from the surfactin class of compounds. This molecular family is highlighted in Figure 2 and shown in more detail in Figure 3. Precursor ions, which matched a molecular networking library standard, are illustrated by diamonds in Figure 3. Indeed, such molecular family contained the ions for surfactin C13 ($[M+Na]^+$ m/z 1030.64), surfactin C14 ($[M+Na]^+$ m/z 1044.66) and surfactin C15 ($[M+Na]^+$ m/z 1058.67). All of these surfactins matched known standards with a cosine score > 0.82 and were mainly detected in both the bacterium and competition extracts (orange node).

Related surfactin derivatives (illustrated by triangles in Figure 3) were also detected in this cluster and displayed a difference of + 18 amu from native surfactins and were assigned as hydrolyzed surfactins (m/z 1048.65 $[C13+Na+H_2O]^+$, m/z 1062.66 $[C14+Na+H_2O]^+$, m/z 1076.68

[C15+Na+H₂O]⁺). Interestingly such compounds were specifically in both the sole bacterium and competition extracts (orange node). In addition, the MS/MS spectrum of the ion detected at m/z 1032.65 (orange node) shows a fragmentation pattern not only similar to that of C14-surfactin but also to a mixture of fragment ions, indicating the presence of several compounds (data not shown). The MS/MS spectrum of the ion detected at m/z 1090.7 (purple node) is similar to that of the hydrolyzed C15-surfactin (m/z 1076.7 [M+Na+H₂O]⁺), but with a mass difference of 14 amu in the b-fragment ion series, indicating that this ion is likely an hydrolyzed C16-surfactin (data not shown). Consequently the two ions detected at m/z 1032.65 and 1076.7 are likely to be surfactin analogs.

Surfactins are cyclic lipopeptides secreted by species of *Bacillus*. The microbial functions described for those compounds include a powerful surfactant effect.³³ Surfactins inhibit the growth and development of other microorganisms by acting primarily on cellular membranes to disrupt membrane integrity.³⁵ Altogether, several studies based on mass spectrometry imaging (MSI) have demonstrated that during bacterial competition, *B. subtilis* is able to produce cyclic surfactant lipopeptides, which inhibit the formation of *Streptomyces* sp. aerial hyphae.³² In addition, MSI measurement undertaken by Dorrestein *et al.*³² in the zone of interaction between *B. subtilis* and *Streptomyces* sp. also revealed the presence of inactive linear surfactins resulting from the hydrolysis of the ester function on the cyclodepsipeptide, suggesting a resistance mechanisms developed by *Streptomyces* against *B. subtilis*.

The morphological aspect of *P. variable* fungal hyphae (Figure 1D) in the course of the interaction with the strain *B. subtilis* as well as the detection of hydrolyzed surfactins in the zone of competition suggest a similar action of surfactins on *P. variable*.

Mass Spectrometry Imaging of the microbial competition between the endophytes *P. variable* and *B. subtilis*.

To explore this hypothesis and map the chemical communication involved in the course of the microbial competition between both endophytes, MSI experiments were performed. Indeed, visualizing microbial interactions with MSI has provided insights into many important biological processes since it allows capturing molecular snapshots of metabolic exchange, antibiotic resistance, and microbial competition.^{29,36,37} There are a number of different MSI methods reported for chemical mapping of microbial systems. Among these, MALDI-MSI has been the most widely used for attaining direct spatial and molecular information of microbial samples.

Sample analysis with MALDI-TOF in positive mode enabled the division of the co-culture area into four regions of interest (ROI), *e.g.* the internal bacterium area, the external bacterium area, the fungus and the competition area. Mass spectra were extracted from each of these ROI corresponding to the bacterium, competition and fungal zones, respectively (Figures 4 and 5). High molecular weight ions were detected in both the bacterium and competition areas (Figure 4), with ions at m/z 1030.6, 1044.7 (C13-, C14-surfactins) especially localized in the bacteria whereas the ions at m/z 1058.7, 1074.7 and 1072.7 (C15-, C16-surfactins) were detected in both competition area and bacterium. Finally, the ions at m/z 1062.7, 1092.7 and 1076.7 (C14, C15 hydrolyzed surfactins) were detected specifically in the competition area. Interestingly, the hydrolyzed C14- and C15-surfactins were almost exclusively detected in the competition area (Figure 4 g-i and Figure 5, ROIs 2 and 3), while native surfactins were mainly detected in the bacterial zone.

Spatial localization of chemical mediators involved in the interspecific microbial competition were also mapped using TOF-SIMS, which is characterized by a better spatial resolution than that of MALDI-TOF.³⁸ Samples do not need to be coated by a matrix when using TOF-SIMS. Samples

prepared on indium tin oxide (ITO) coated glass slides and silicon wafer yielded no results as the printing disturbed the distribution of the allelochemicals. In addition, the fungal morphology was greatly modified in the presence of ITO. Alternatively, growing the microorganisms on filter paper covering the MEA agar medium allowed maintaining a strong antibiosis without disturbing the other biological processes. Furthermore, the surface is flatter using the paper filter which removed the topography of the fungal mycelium (Figure S1). The TOF-SIMS analysis of the endophytic competition was thus made at two different growing distances (1.5 and 2.5 cm). This enabled the analysis of different ROIs as shown in Figure 6 and Figure 7. The growing distance of 2.5 cm showed the native C15-surfactin (m/z 1034.7 [M-H]⁻, (red color in Figure 7, ROI 1) was exclusively localized in the bacterium area while the hydrolyzed C15-surfactin (m/z 1052.7 [M-H]⁻, green color in Figure 6, ROI 3) was confined to the competition area.

Interestingly, the data from the growing distance of 1.5 cm showed additional hydrolyzed surfactins that were detected, such as C13- and C14-surfactins at m/z 1024.7 and 1038.7, respectively (Figure 7). The analysis with TOF-SIMS of the same samples but in positive mode confirmed these observations (data not shown).

Thus, both MALDI-TOF and TOF-SIMS imaging allowed the detection of hydrolyzed surfactins in the course of the interspecific endophytic microbial competition. In addition, such MSI results are also in accordance with the Orbitrap MS/MS data and Molecular Networking representation which showed the presence of hydrolyzed surfactins in the competition area extract and suggested the excretion of a putative fungal protein related to hydrolase as previously described for the detoxification process by *Streptomyces*.³²

Enzymatic degradation or modification have been well described in the context of antibiotic resistance.³⁹ Degradative enzymes that impact competitive interactions also include those that

degrade metabolites with signaling functions. Such mechanisms have been extensively described for bacteria but are less common for fungi except for pathogenic strains, which developed diverse responses to counteract the arsenal of host-plants allelopathic metabolites.^{40,41} In the case of endophytes, recent studies have highlighted the potential of endophytic fungi for the production of new compounds through the biotransformation of natural products.⁴²⁻⁴⁷ Nevertheless, these studies are not ecologically relevant. In addition, previous work by our research group has highlighted the ability of the endophytic fungus *P. variable* to metabolize natural products such as polyketides or flavonoids which may be related to the host plant.^{11,12}

Biotransformation of the surfactins by the fungus *P. variable*.

In order to assess the resistance capacity of *P. variable* against *B. subtilis* surfactant lipopeptides, a commercially available surfactin was added to the fungal biomass in biotransformation experiments as previously described for other compounds.¹² The hydrolysis of surfactins in the presence of the fungal biomass was monitored by UPLC-MS (Figure S5). After 24 hours of being in contact with the fungal biomass, native C14- and C15-surfactins disappeared entirely while hydrolyzed C14- and C15-surfactins were detected. Control consisting of surfactin alone in the buffer was also performed and no hydrolyzed surfactin was detected. Such experiments were also performed in the sole presence of the culture supernatant, and similar metabolites profiles were observed suggesting that fungal secreted enzymes are involved in these reactions (data not shown).

Antimicrobial compounds produced by *P. variable*.

As previously highlighted in this study by molecular networking and MSI, several metabolites were produced by the fungus *P. variable* and were detected in the competition area. None of the fungal metabolites matched known natural products within the searched databases. Therefore, the metabolites produced by *P. variable* that inhibited *B. subtilis* were isolated from the crude extract using bioactivity-guided fractionation. Compound **1**, a colorless crystalline solid with an $[\alpha]_D^{20}$ of + 63.3 (*c* 0.3, CHCl₃), was found to be one of the main compounds inhibiting the growth of *B. subtilis*. The molecular formula C₁₅H₁₈O₄ indicating seven degrees of unsaturation was deduced from the molecular peak at *m/z* 261.1110 (calc. 261.1127) [M-H]⁻ in ESI-HRMS. The infrared spectrum pointed out the presence of carbonyl groups (1747 and 1717 cm⁻¹). The ¹H NMR spectrum of **1** showed signals for three methyl groups at δ_H 1.00 (3H, H-6', t, *J* = 7.4), δ_H 1.61 (3H, s, H-7), 2.10 (3H, H-3'', dd, *J* = 7.1, 1.6), six olefinic protons [δ_H 5.55 (1H, d, *J* = 15.5 Hz, H-1'), 5.87 (1H, dd, *J* = 15.1, 6.5 Hz, H-4'); 6.00 (1H, dd, *J* = 15.1, 10.5 Hz, H-3'), 6.29 (1H, dd, *J* = 15.5, 10.6 Hz, H-2'), 7.37 (1H, dd, *J* = 15.7, 1.6 Hz, H-1''), 7.37 (1H, qd, *J* = 15.7, 7.1 Hz, H-2'')] and one methylene 2.10 (1H, m, H-5'). The ¹³C NMR spectrum of **1** displayed three sp³ methyl (δ_C 13.1, 19.5, 22.0), one sp³ methylene (δ_C 25.6) in addition to one sp³ quaternary carbon (δ_C 91.8). This one showed also ten sp² carbons (including six methines at δ_C 120.3, 124.1, 127.4, 133.0, 140.5, 148.3, two carbonyls at δ_C 203.8, 185.7, an oxygenated carbon at δ_C 185.7 and one quaternary carbon). In addition *E* configurations were assigned for the double bonds by analysis of coupling constants.

The data analysis of 2D NMR spectra (including COSY, HSQC, HMBC, Figure 8) revealed that **1** is a (2*H*)furan-3-one identified as the known compound nivefuranone A, previously isolated from the endophytic fungus *Microdiplosia* sp. KS75-1.⁴⁸ Absolute configuration at C-5 was

suggested as *S* because of its positive rotation value which is in accordance with aspertetronin A⁴⁹ and is found the opposite to that of gregatine A.^{50,51}

Inhibition of the growth of *B. subtilis* in the presence of nivefuranone A was performed in solid media and 96-wells plates with resazurin coloration. In both cases a potent inhibition was observed compared with the control (Figure 8, CMI: 76 μ M) suggesting that nivefuranone A is one of the fungal metabolites involved in the competition between these two endophytes. It should be noted that compound (**1**) has not been detected by MSI analysis, probably because of its poor ionization.

CONCLUSION

Deciphering the molecular mechanism involved in interspecific microbial competition has attracted growing interest in this last decade.⁵²⁻⁵⁴ However, few studies focused on interspecific communication between endophytic microorganisms evolving from the same plant host. As a result, the molecular basis of endophytic interactions is not well understood although it is now well established that endophyte communities directly or indirectly interacts within the plant (fungus-fungus or fungus-bacterium interaction). In this plant microbiota, potentially every natural product could have an impact on the metabolic and transcriptomic profiles of the neighbour microorganisms.^{55,56}

Visiting the remarkably multifarious group of endophytes through their antibiosis interactions in the host-plant microbiota provided several opportunities to understand the functions and identity of signaling molecules and improve our understanding of the chemical language between endophytic bacteria and fungi. In this study, the chemical communication between the fungus *P. variable* and the bacterium *B. subtilis*, both isolated from the leaf of the conifer *C. harringtonia*, was examined by multidisciplinary tools including molecular networking and

MSI. This work enabled the detection of lipopeptide surfactins produced by *B. subtilis*, which are well known for their "balding effect" (surfactant activity) toward their microbial competitors, also likely to explain the morphological changes observed on *P. variable* hyphae. In response to this challenge, it was demonstrated through biotransformation studies and MSI that *P. variable* may resist to the bacterial assault by hydrolyzing the surfactins. In addition, *P. variable* was found to produce (2*H*) furan-3-one with an antibiotic effect, identified as nivefuranone A and likely to prevent the growth of the bacterium.

This study shows that MSI is a powerful tool to identify and map *in situ* the production of chemical mediators present in very limited amounts. Moreover, its combination with other analytical methods, such as molecular networking, empowers microbial natural products chemistry enabling rapid detection of metabolites involved in microbial communication.

EXPERIMENTAL SECTION

Competition between endophytic microorganisms

The fungus *Paraconiothyrium variable* strain LCP5644 (MNHN collection) and the bacterium *Bacillus subtilis* strain 9E1a were isolated from the inner tissue of the needle of *Cephalotaxus harringtonia* var. *drupacea* (reference N°2686 Arboretum de Chèvreloup MNHN). Endophytic microorganisms were cultivated on solid medium MEA (malt extract 20 g/L, glucose 20 g/L, bacteriological peptone 1 g/L, and purified agar CONDA 20 g/L). Competition experiments were performed in Petri dishes (12 cm², MEA 60 mL) by setting 10 µL of each microbial suspension at 1.5 and 2.5 cm distantly from each other. The cultures were incubated at 24 °C under ambient light. Monocultures of fungi and bacteria were performed as controls also in triplicate. To exclude

the involvement of volatile organic compounds, the competition was also assessed in Petri dish (9 cm², MEA 25 mL) divided by a plastic barrier.

Mass spectrometry analysis

The medium extracts were characterized by online nano-LC and electrospray tandem mass spectrometry. The analyses were performed on a U3000 Dionex nanoflow system connected to a LTQ Orbitrap mass spectrometer equipped with a nano-electrospray source (Thermo-Fischer, Les Ulis, France). Chromatographic separation took place in a C18 pepmap 100 column (75 μm ID, 15 cm length, 5 μm, 10 nm, Dionex). The extracts were injected on pre-concentration column with a flow rate of 20 μL.min⁻¹ of water/TFA (0.1 %). After three minutes of wash with the same solvent, the compounds were eluted and separated in the analytical column with a flow of 200 nL/min and a gradient from 2 % to 60 % acetonitrile with 0.1 % formic acid in 30 minutes. The mass spectrometer was operated in the data dependent mode to automatically switch between Orbitrap MS and MS² in CID mode in the linear trap. Survey full scan MS spectra from *m/z* 200 to *m/z* 1500 were acquired in the Orbitrap with mass resolution of 30 000 at *m/z* 400, after accumulation of 500 000 charges in the linear ion trap. The most intense ions (up to four, depending on signal intensity) were sequentially isolated for fragmentation, in the linear ion trap using CID at a target value of 100 000 charges. The resulting fragments were recorded in the Orbitrap with a mass resolution of 7 500.

Molecular networking of competition between endophytic microorganisms

HR-MS/MS raw data files were converted from .RAW to .mzXML file format using the Trans-Proteomic pipeline (Institute for Systems Biology, Seattle)⁵⁷ and molecular networking were created using the online workflow at Global Natural Products Social (GNPS)^{58,59} (gnps.ucsd.edu).⁶⁰ The data were then clustered with MS-Cluster with a parent mass tolerance of

0.2 Da and a MS/MS fragment ion tolerance of 0.1 Da to create consensus spectra. Further, consensus spectra that contained less than 2 spectra were discarded. A network was then created where edges were filtered to have a cosine score above 0.7 and more than 6 matched peaks. Further edges between two nodes were kept in the network if and only if each of the nodes appeared in each other's respective top 10 most similar nodes. The spectra in the network were then searched against GNPS's spectral libraries. To visualize the data, they were imported into Cytoscape software (version 3.2.1)⁶¹ where nodes correspond to a specific consensus spectrum (parent mass ions) and edges represent significant pairwise alignment between nodes (cosine score ranging from 0 to 1 (identical fragmentation spectra)).

Sample preparation for mass spectrometry imaging

The competition was performed on a MALDI plate (MTP 384 plate polished steel BC, Bruker Daltonique, Wissembourg, France) by applying a thin layer of MEA (5 mL). Once the agar solution cooled, 2 μ L of bacterial suspension (10^4 cells/mL) and 5 mL of mycelial suspension (50 mm³ mycelium pieces vortexed and sonicated in 1 mL of sterile water) were deposited at 1.5 or 2.5 cm apart from each other. For TOF-SIMS experiments, a round Petri dish (9 cm²) was filled with 15 mL of MEA medium and once cooled, sterilized filter paper (Qualitative, Number 2, Cat. No 1002125 WhatmanTM) was gently deposited on the medium. A volume of 10 μ L of the previous microbial suspension was deposited at a distance of 1.5 or 2.5 cm. Competitions on silicon wafer and ITO coated glass slides were also assessed. All the cultures were incubated at 24 °C for 26 days under ambient light. Optical images of the samples were recorded with an Olympus BX51 microscope (Rungis, France), equipped with 1.25 \times to 50 \times lenses and a SC30 camera, monitored by Stream Motion 1.9 software (Olympus, Rungis, France).

Matrix coating and MALDI-TOF Imaging

CHCA matrix solution was prepared in ACN/H₂O/TFA (70/30/0.1 *V:V:V*) at 10 mg·mL⁻¹, and then deposited on the agar surface with a TM-Sprayer (HTX Technologies, Carrboro, NC, USA) at 70 °C, with movement speed of 120 cm/min, nebulized nitrogen pressure of 10 psi (~700 hPa) and pump flow rate of 0.24 mL·min⁻¹. The samples on MALDI plate were analyzed with a MALDI-TOF/TOF UltrafleXtreme (Bruker Daltonique, Wissembourg, France) mass spectrometer in reflector mode and MS/MS fragmentation was performed on both samples and commercial surfactins control. Frequency of the Smartbeam-IITM Nd:YAG (wavelength 355 nm) laser was set at 2 kHz while the laser power was adjusted according to signal intensity. Shot number per pixel was set to 500 and pixel size to 150 microns. After a delay of 210 ns, the ions produced were extracted and then accelerated with a voltage of 25 kV. This setting allowed the measurement of a mass resolution of 36 000 for the monoisotopic peak corresponding to protonated bradykinin at *m/z*1060.57. Mass calibration was carried out using 4 peaks of PepMix 5 (bradykinin [1-5], *m/z* 573.31; bradykinin [1-7], *m/z*757.40; bradykinin, *m/z*1060.57; and angiotensin, *m/z* 1296.68), with a "Quadratic / Cubic Enhanced" algorithm. Average mass accuracy of 3.8 ppm was thus measured on these standards. Acquisitions and image reprocessing (ion density maps) were performed with flexControl 3.4 and flexImaging 4.0 software (Bruker Daltonique, Wissembourg, France), respectively. The component spectra were normalized using the "median" method to avoid normalization-induced artifacts.⁶²

TOF-SIMS Imaging

After the cultivation, the filter paper on which the bacteria and fungi were co-cultured was removed from the Petri dish and dried under vacuum for at least 3 h to remove the moisture absorbed from culture media. A small rectangular piece of the filter paper containing fungi and bacteria was then cut off followed by being fixed on a stainless steel plate by conductive double-

sided tape. The fungi were previously removed from the filter paper to avoid topographic effect on the surface and contamination into the mass spectrometer.

TOF-SIMS imaging acquisitions were recorded with a commercial TOF-SIMS IV (ION-TOF GmbH, Münster, Germany) single stage reflectron TOF mass spectrometer. The primary ion beam is of Bi_3^+ cluster ions delivered by a bismuth liquid metal ion gun (LMIG) with a kinetic energy of 25 keV. The so-called high current bunched mode (described in detail elsewhere)⁶³ was utilized to focus and accelerate the ion beam to guarantee a high mass resolution, providing a pulsed primary ion current of ~ 0.4 pA at 10 kHz. Secondary ions are extracted and first accelerated to a kinetic energy of 2 keV and then post-accelerated to 10 keV before hitting a hybrid detector composed of a single micro-channel plate followed by a scintillator and a photomultiplier. Large area analyses were realized by moving the sample stage step by step with a patch size of $500 \mu\text{m} \times 500 \mu\text{m}$, a pixel density of 100×100 pixels and 10 pulses per pixel, resulting in an ion dose density of $\sim 1.0 \times 10^{10}$ ions $\cdot\text{cm}^{-2}$. A low energy (21 eV) pulsed electron flood gun was applied during the acquisitions to compensate for the charges accumulated on the surface of the insulating sample. Thanks to the linear function of time-of-flight and the square root of m/z , mass spectra were calibrated with internal low mass fragments: C^- , CH^- , C_2^- , C_3^- , and C_4H^- in negative ion mode. Data acquisition and processing were performed using SurfaceLab 6.5 software (ION-TOF GmbH, Münster, Germany).

Nano-Spray-Orbitrap MS/MS of competition extract

The filter paper corresponding to the competition zone was cut off and washed with 100 μL ethanol. After being vortexed for 30 min, the filter paper which was immersed in ethanol was stored at -20 °C overnight. Then the supernatant was dried by a vacuum concentrator, followed by being dissolved with 5 μL ethanol solvent to obtain the final stock solution. For MS/MS

experiment, 1 μL stock solution was diluted in 4 μL spray solvent (ACN/H₂O/FA, 50/50/0.5 *V/V/V*) and all the 5 μL solution was loaded into a nano-capillary needle (Thermo Fisher Scientific, Le Ulis, France).

Fungal biotransformation experiments

P. variable was cultivated in YMS medium (glucose 16 $\text{g}\cdot\text{L}^{-1}$, yeast extract 4 g/L , malt extract 10 g/L , bacteriological peptone 5 g/L) by inoculating spore suspension (2 cm^2 plug in 1 mL of 20 % glycerol solution, filtered through a miracloth of 25 μm , final concentration 10^6 spores/mL). 500 μL of this suspension was added to 50 mL YMS medium in a 150 mL Erlenmeyer flask. Fungal biomass was obtained after 72 hours of incubation at 27 °C under mild rotary shaking (160 rpm). The collected biomass was filtered, yielding 1.5 g of fungal mycelium which was stored in phosphate buffer (4 mL, pH 6). 4 μL of commercial surfactin solution (DMSO, 20 $\text{mg}\cdot\text{mL}^{-1}$) was added to *P. variable* biomass while controls were carried out by adding 40 μL of surfactin solution to phosphate buffer solely and 40 μL of DMSO to *P. variable* biomass, respectively. After 24 hours, 300 μL of methanol was added to 1.5 mL of mycelia and supernatant, sonicated for 20 minutes, centrifuged and 10 μL of supernatant was injected into UPLC-MS to detect hydrolyzed surfactins.

Fermentation, Extraction, and Isolation. Spore suspension of *P. variable* (10^6 spores/mL) was spread on fifteen Petri dishes with Malt Extract agar medium and incubated at 25 °C for 26 days. Following this fermentation, the mycelium and the broth were extracted with ethyl acetate (3 times). The combined organic phases were dried over Na₂SO₄, filtered and concentrated *in vacuo* to afford 900 mg of crude extract.

The EtOAc extract of *P. variabile* obtained was purified by preparative HPLC (gradient from 45 % to 52 % MeCN in H₂O for 32 min; flow rate: 20.0 mL·min⁻¹; t_R = 28.5 min) to yield nivefuranone A (**1**).

Antimicrobial activity of nivefuranone A.

The antibacterial activity of nivefuranone A and fungal crude extract were evaluated using the agar diffusion. Briefly, culture suspension of *B. subtilis* 9E1a (approximately 10⁶ CFU/mL) was spread on the solid medium plates (40 mL). Ten microliters of nivefuranone A (DMSO, 50 and 10 mg/mL) and 10 µL the fungal crude extract (DMSO, 50, 10 and 1 mg·mL⁻¹) were deposited onto the solid media plates. The diameter of inhibition zone was measured after 48 h of incubation at 25 °C. Econazole (10 µL, 5 mg/mL) and DMSO were used as positive and negative controls respectively.

Minimum Inhibitory Concentration (MIC) of Nivefuranone A.

MICs were determined using the microdilution resazurin assay. Resazurin salt powder (Sigma) was prepared in distilled water (0.01 %, w/v), sterilized by filtration through a 0.22 µm membrane, and stored at 4 °C for a week.

The inoculum was prepared from *B. subtilis* cultivated in Luria-Bertani medium for 24 hours. Two microliters of nivefuranone A (10 mg/mL in DMSO) were added in 200 µL of LB medium and serial dilutions were performed in 96-well plates at concentrations from 100 to 0.1 µg/mL. Growth controls containing DMSO and chloramphenicol (from 1 µg/mL to 1 ng/mL) were also included. The plates were incubated at 26 °C. After 2 days, 30 µL of resazurin solution was added to each well and plates were allowed to incubate at 37 °C for an additional 24 h. A change from blue to pink indicates reduction of resazurin and therefore bacterial growth. The MIC was defined as the lowest drug concentration that prevented this colour change.

ASSOCIATED CONTENT

Supporting Information. Additional experimental details are disclosed. This supporting information is available free of charge via the Internet at <http://pubs.acs.org>.

AUTHOR INFORMATION

Corresponding Authors

*Alain.Brunelle@cnrs.fr. Tel : +33 169 824 575

*sprado@mnhn.fr. Tel.: +33 1 40 79 31 19.

Notes

The authors declare no competing financial interest.

ACKNOWLEDGMENT

The 400 MHz and 600 MHz NMR spectrometers used in this study were funded jointly by the *Région Ile-de-France*, the MNHN (Paris, France) and the CNRS (France). The Muséum National d'Histoire Naturelle (MNHN) is acknowledged for research funding (the *Action Transversale du Muséum* « Biodiversité des Microorganismes dans les Ecosystèmes Actuels et Passés »).

The UltrafleXtreme MALDI TOF/TOF mass spectrometer used in this study was funded by a grant from the *Région Ile-de-France* and the CNRS-ICSN (DIM Analytics Equipements Mi-Lourds 2012).

Q.P.V. is indebted to the « Fondation pour le développement de la chimie des substances naturelles et ses applications » for a Ph.D. research fellowship. We acknowledge the sponsorship from Chinese Scholarship Council (CSC) for T.F. Ph.D. study (No. 201406310013). This work

has benefited from an “Investissement d’Avenir” grant managed by Agence Nationale de la Recherche (CEBA, ref. ANR-10-LABX-25-01).

Authors would also like to acknowledge Didier Buisson for fruitful discussions about surfactins biotransformations.

Author Contributions

The manuscript was written through contributions of all authors. All authors have given approval to the final version of the manuscript. ‡These authors contributed equally

Funding Sources

Any funds used to support the research of the manuscript should be placed here (per journal style).

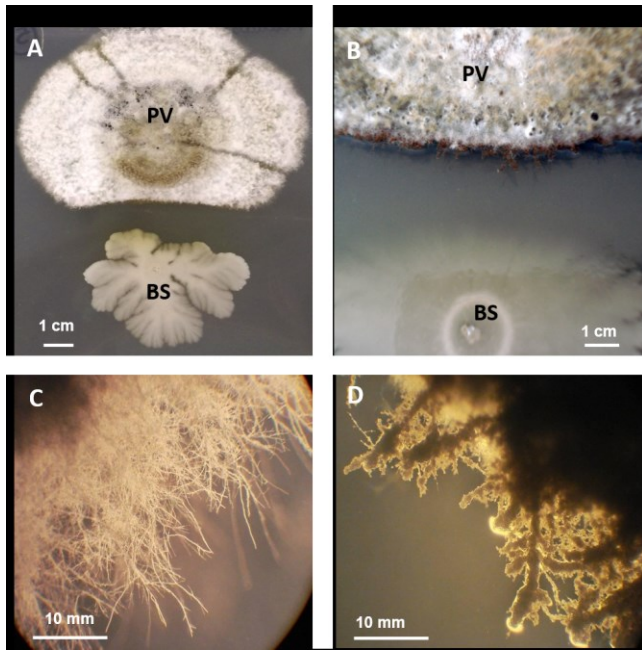


Figure 1. A) Antagonism between the fungus *P. variable* (PV) and the bacterium *B. subtilis* (BS) on solid medium at 20 days post-inoculation. B) Zoom on the fungal hyphae in the course of the competition between the two endophytes. C) Observation of *P. variable* hyphae in monoculture and D) in the course of the competition.

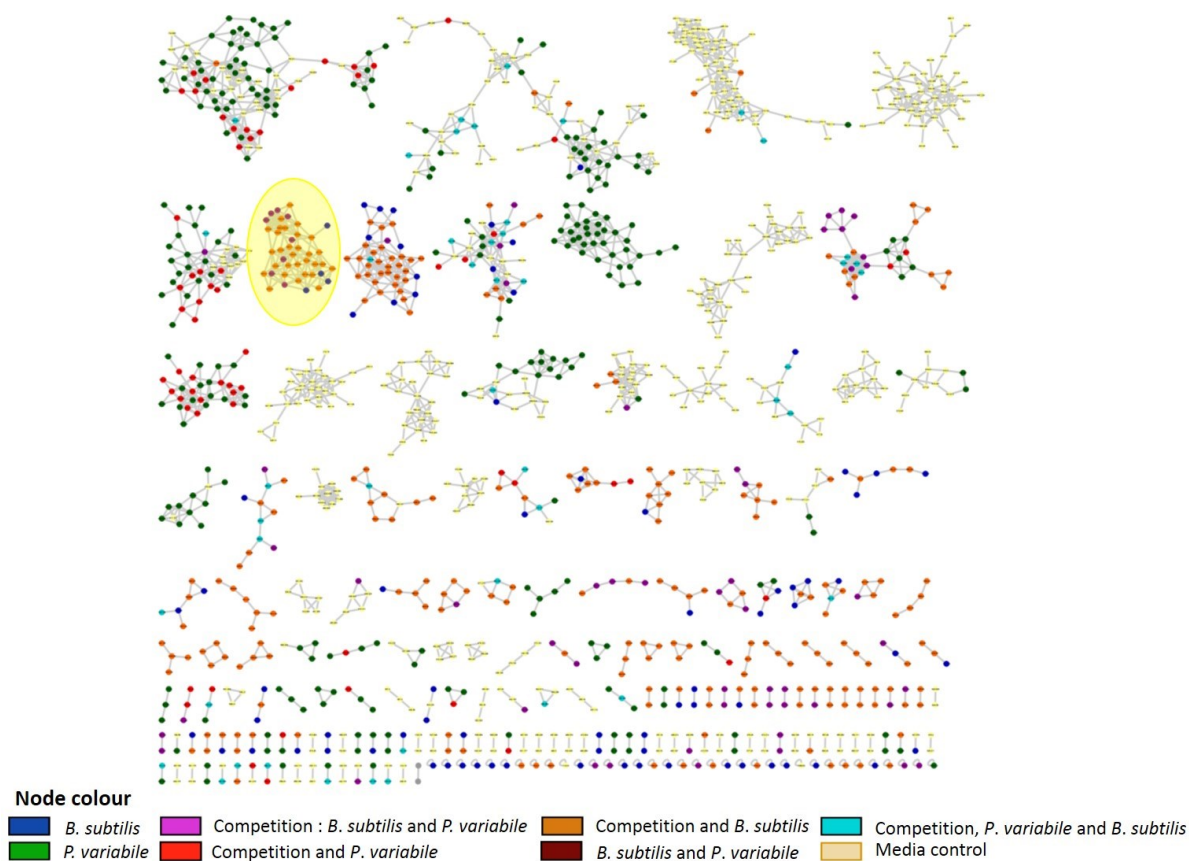


Figure 2. Molecular network of 2672 precursor ions from crude extracts of *B. subtilis* 9E1a (blue nodes), *P. variable* (green nodes) and a competition interaction between the two strains (purple nodes). Precursor ions produced by both *B. subtilis* and *P. variable* monocultures but not present during the interaction (maroon nodes), precursor ions produced by *B. subtilis* and present during the competition interaction (orange nodes), precursor ions produced by *P. variable* and present during the competition interaction (red) and precursor ions present under all three culture conditions (light blue) are also present. Precursor ions obtained from the media control are colored yellow.

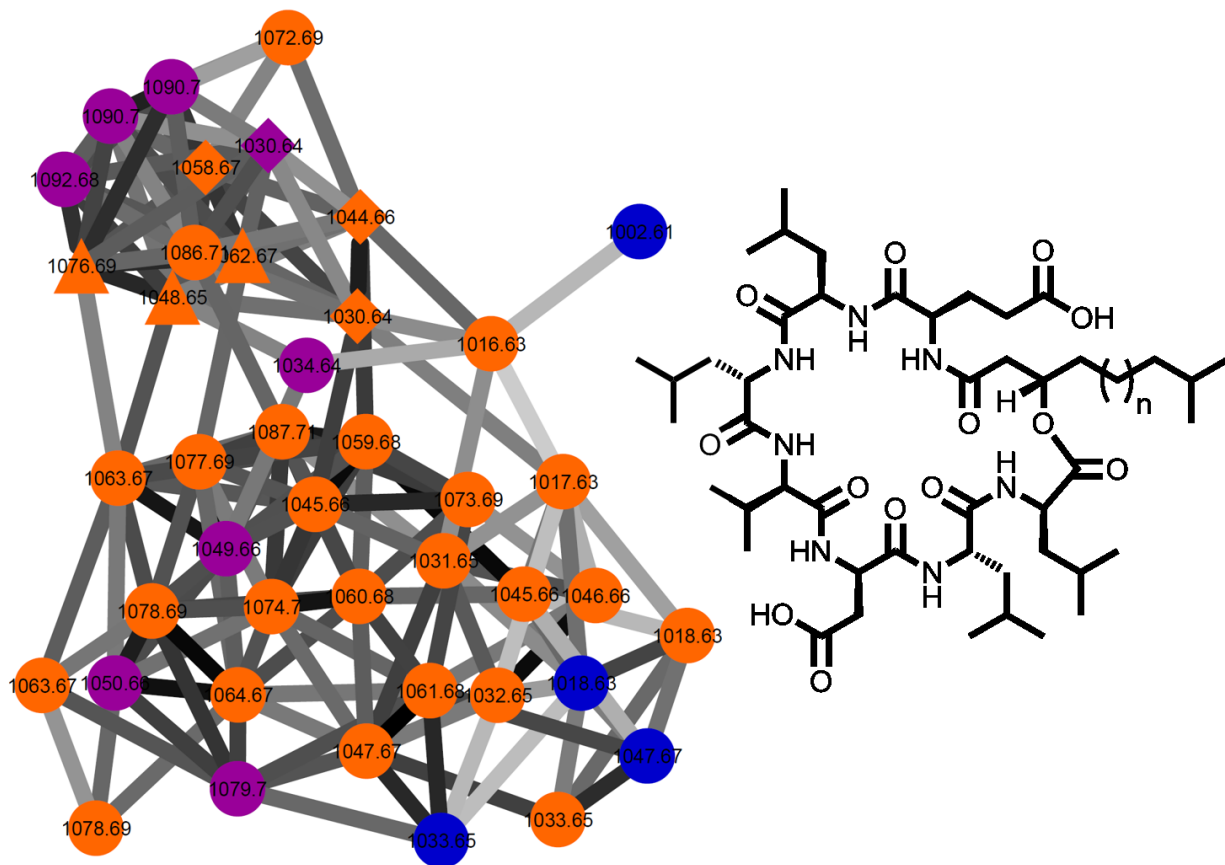


Figure 3. A) Surfactin molecular family (highlighted yellow in the molecular network in Figure 2). Nodes are color coded as depicted in Figure 2. If parent ions matched molecular network library standards, they are labelled as diamonds: m/z 1030.64, C13-surfactin $[M+Na]^+$; m/z 1044.66, C14-surfactin $[M+Na]^+$; m/z 1058.67, C15-surfactin $[M+Na]^+$. Specific hydrolyzed surfactins are represented with triangles: m/z 1048.65, hydrolyzed C13-surfactin $[M+Na+H_2O]^+$; m/z 1062.66, hydrolyzed C14-surfactin $[M+Na+H_2O]^+$; m/z 1076.68, hydrolyzed C15-surfactin $[M+Na+H_2O]^+$; m/z 1092.68. Withdrawal of the edge is related to the cosine score (from grey, cosine score: 0.7, to black, cosine score: 1). B) chemical structure of surfactins (n=5, C13-surfactin; n=6, C14-surfactin; n=7, C15-surfactin).

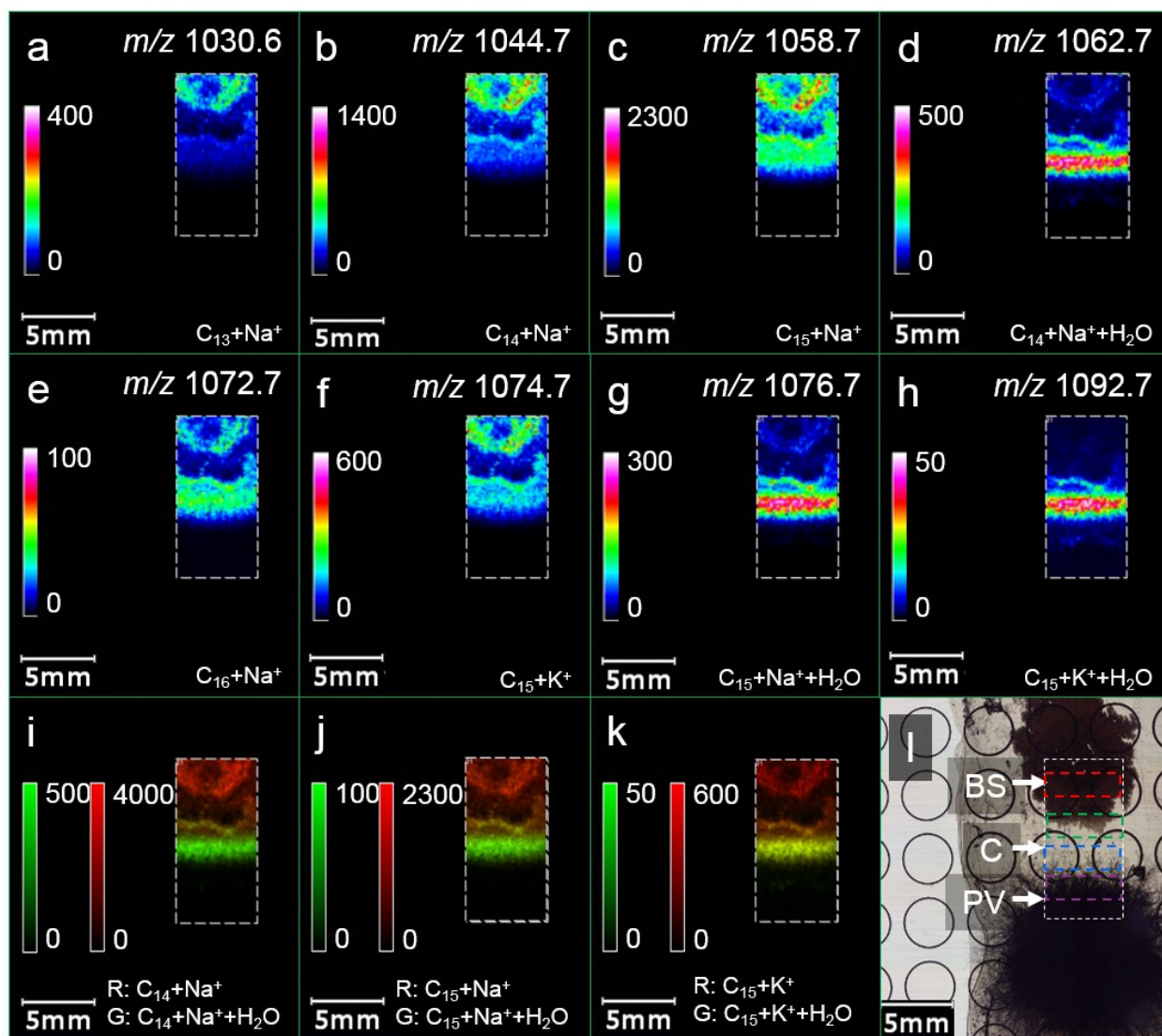


Figure 4. MALDI-TOF ion images of surfactins and hydrolysed surfactins produced during competition with a growing distance of 1.5 cm (a) m/z 1030.6 C_{13} -surfactin $[M+Na]^+$. (b) m/z 1044.7 C_{14} -surfactin $[M+Na]^+$. (c) m/z 1058.7 C_{15} -surfactin $[M+Na]^+$. (d) m/z 1062.7 Hydrolysed C_{14} -surfactin $[M+Na]^+$. (e) m/z 1072.7 C_{16} -surfactin $[M+Na]^+$. (f) m/z 1074.7 C_{15} -surfactin $[M+K]^+$. (g) m/z 1076.7 Hydrolysed C_{15} -surfactin $[M+Na]^+$. (h) m/z 1092.7 hydrolysed C_{15} -surfactin $[M+K+H_2O]^+$. (i) Two-color overlay of sodium cationized C_{14} -surfactin $[M+Na]^+$ and hydrolysed C_{14} -surfactin $[M+Na]^+$. R: Red; G: Green. (j) Two-color overlay of sodium cationized C_{15} -surfactin $[M+Na]^+$ and hydrolysed C_{15} -surfactin $[M+Na]^+$. R: Red; G: Green. (k) Two-color

overlay of potassium cationized C₁₅-surfactin [M+K]⁺ and hydrolysed C₁₅-surfactin [M+K]⁺. R: Red; G: Green. (l) Optical image of *B. subtilis* (BS) and *P. variabile* (PV) co-cultured on a MALDI target plate with an inoculating distance of 1.5 cm. The analyzed area is highlighted by a white dotted rectangular. The four dotted color squares correspond to four ROIs, of which the size of each is 407 pixels. “C” corresponds to competition zone between BS and PV.

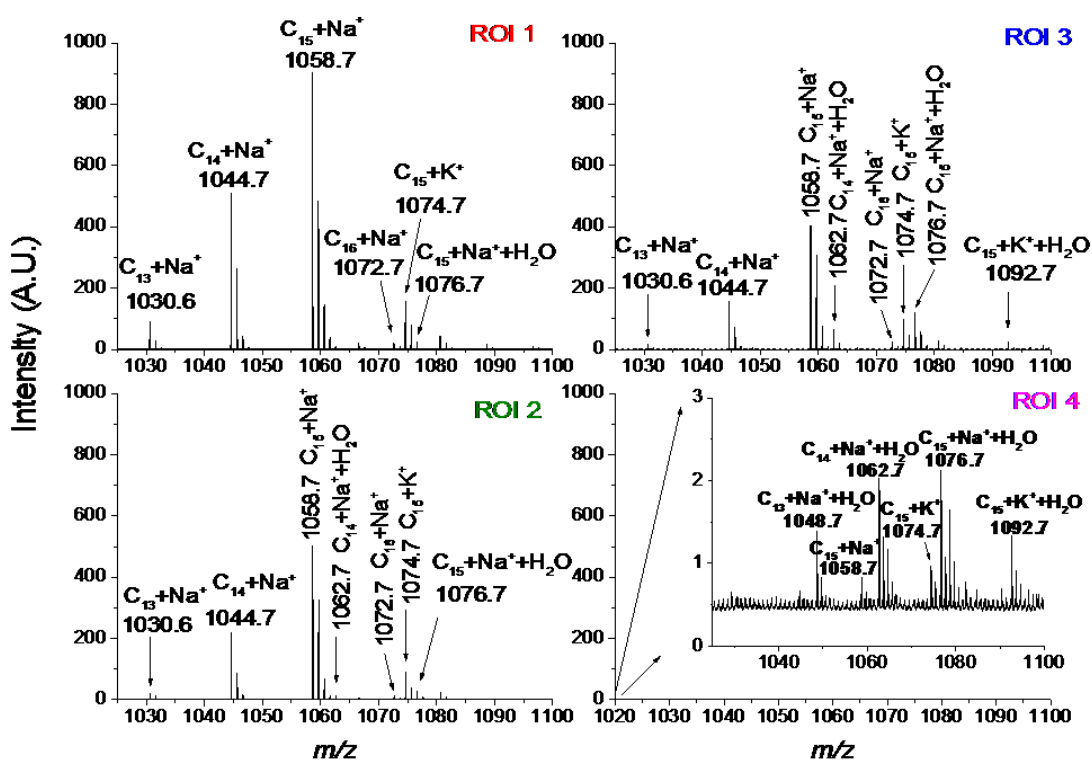


Figure 5. MALDI-TOF mass spectra from the four ROIs indicated in Figure 4. ROI 1 corresponds to the *B. subtilis* zone; ROI 2 corresponds to the end of *B. subtilis* zone and the beginning of the

competition zone; ROI 3 corresponds to the competition zone; ROI 4 corresponds to the *P. variabile* zone.

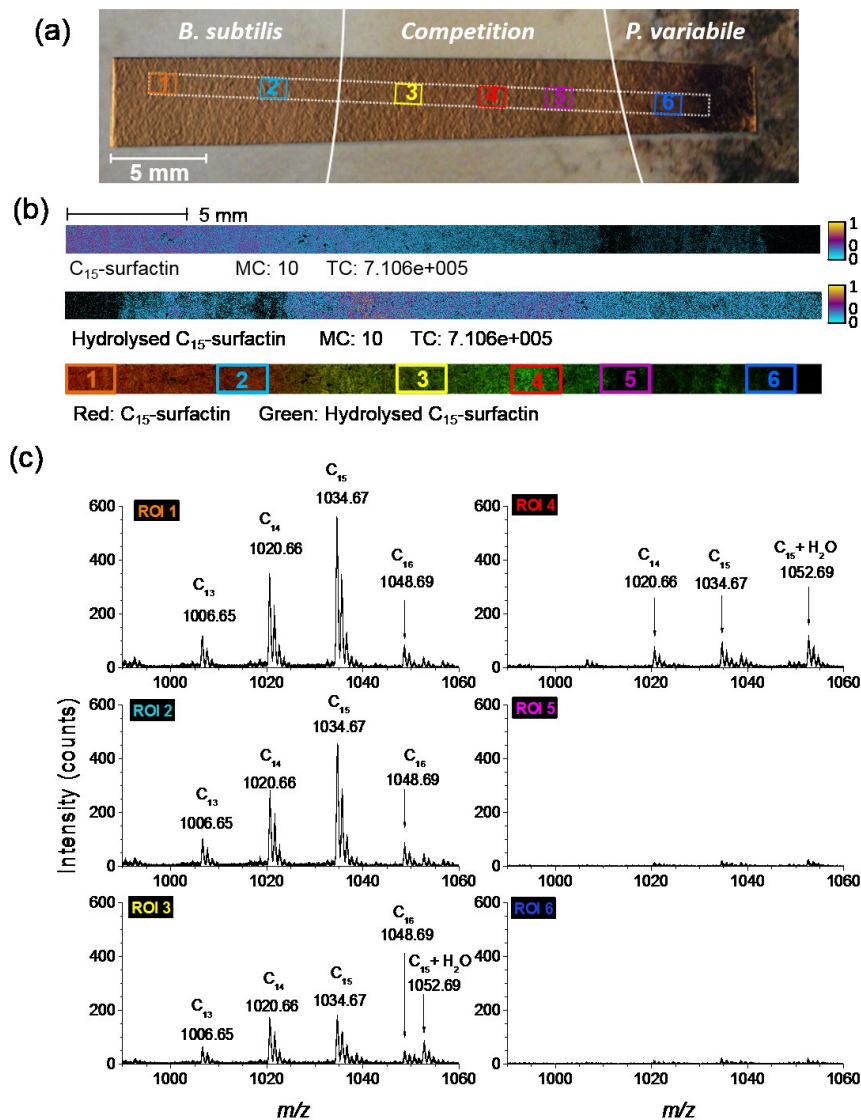


Figure 6. TOF-SIMS imaging of surfactin and hydrolyzed surfactin distribution with a growing distance of 2.5 cm. (a) Optical image of filter paper on which *B. subtilis* and *P. variabile* were co-cultured. (b) Ion images of C_{15} -surfactin, hydrolyzed C_{15} -surfactin, and a two-color overlay between these two compounds. The six colored rectangles correspond to six regions of interest

(ROIs). (c) Mass spectra of the six ROIs. The analyzed area is 30 mm × 1 mm while the size of each ROI is 1.5 mm × 1 mm.

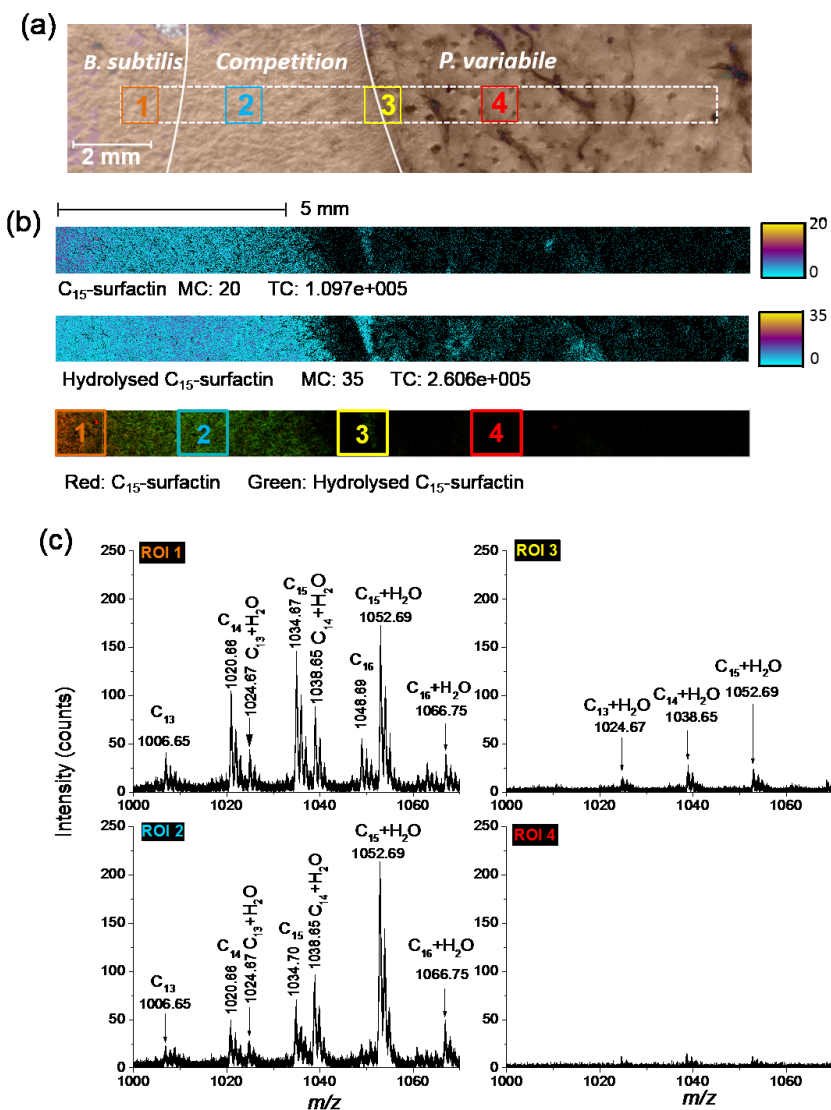


Figure 7. TOF-SIMS imaging of surfactin and hydrolyzed surfactin distribution with growing distance of 1.5 cm. 15 mm × 1 mm. (a) Optical image of filter paper on which *B. subtilis* and *P. variabile* were co-cultured. (b) Ion images of C_{15} -surfactin, hydrolyzed C_{15} -surfactin, and a two-color overlay between these two compounds. The four squares correspond to four regions of

interest (ROIs). (c) Mass spectra of the four ROIs. The analyzed area is 15 mm × 1 mm while the size of each ROI is 1 mm × 1 mm.

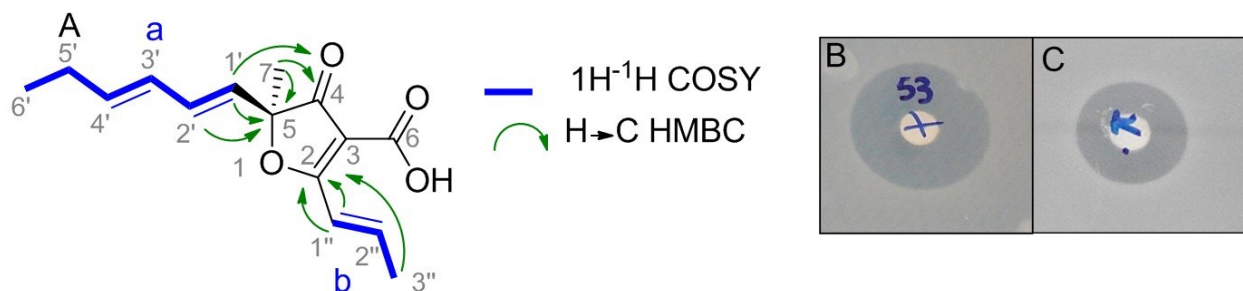
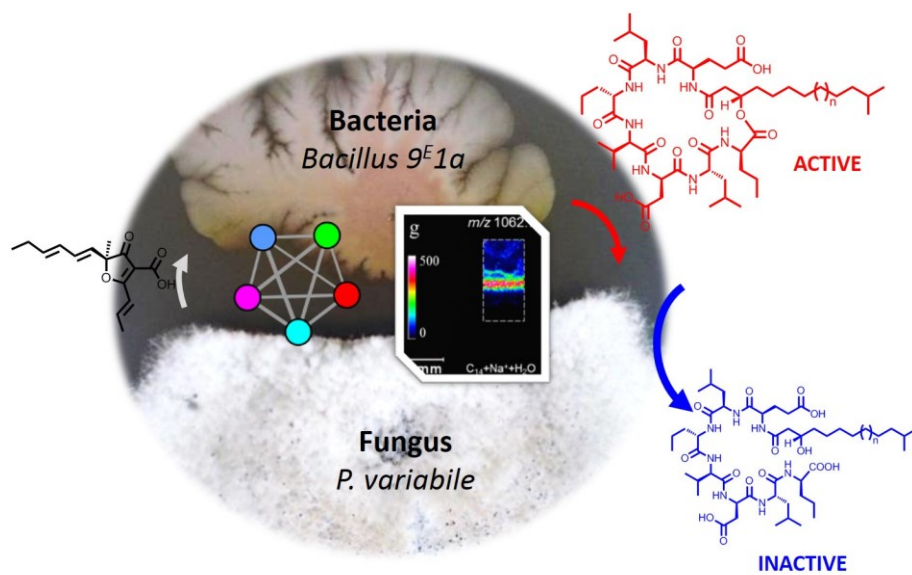


Figure 8. Main compound isolated from *P. variable* and inhibiting the growth of the bacterium *B. subtilis*. A) Structure of the nivefuranone A (compound 1) and key HMBC and COSY correlations. B) and C) Antimicrobial activity against *B. subtilis* in the presence of nivefuranone A and kanamycin, respectively.

Insert Table of Contents Graphic and Synopsis Here



REFERENCES

- (1) Kues, U.; Navarro-Gonzalez, M. In *Physiology and genetics, 1st edition, The Mycota XV*; Anke, T., Weber, D., Eds.; Springer: 2009, p 79.
- (2) Leeder, A. C.; Palma-Guerrero, J.; Glass, N. L. *Nature Rev. Microbiol.* **2011**, *9*, 440.
- (3) Bacon, C.; W.; White, J., L.F.; Eds. of *Microbial Endophytes*, Marcel Dekker, Inc.: New York, 2000.
- (4) Kusari, S.; Spiteller, M. *Nat. Prod. Rep.* **2011**, *28*, 1203.
- (5) Prado, S.; Li, Y.; Nay, B. In *Studies in Natural Products Chemistry*; Atta-Ur-Rahman, Ed. 2011, 249-296.
- (6) Langenfeld, A.; Prado, S.; Nay, B.; Porcher, E.; Cruaud, C.; Lacoste S.; Bury, E.; Hachette, F.; Hosoya, T.; Dupont, J. *Fungal Biol.* **2013**, *117*, 124.
- (7) Abdelkafi, H.; Nay, B. *Nat. Prod. Rep.* **2012**, *29*, 845.
- (8) Evanno, L.; Jossang, A.; Nguyen-Pouplin, J.; Delaroche, D.; Herson, P.; Seuleiman, M.; Bodo, B.; Nay, B. *Planta Med.* **2008**, *74*, 870.
- (9) Bocar, M.; Jossang, A.; Bodo, B. *J. Nat. Prod.* **2003**, *66*, 152.
- (10) Combes, A.; Ndoye, I.; Bance, C.; Bruzard, J.; Djediat, C.; Dupont, J.; Nay, B.; Prado, S. *PloS one* **2012**, *7*, e47313.
- (11) Tian, Y.; Amand, S.; Buisson, D.; Kunz, C.; Hachette, F.; Dupont, J.; Nay, B.; Prado, S. *Phytochemistry* **2014**, *108*, 95.

- (12) Prado, S.; Buisson, D.; Ndoye, I.; Vallet, M.; Nay, B. *Tetrahedron Lett.* **2013**, *54*, 1189.
- (13) Somjai peng, S.; Medina, A.; Kwasna, H.; Ordaz Ortiz, J.; Magan, N. *Fungal Biol.* **2015**, *119*, 1022.
- (14) Reinhold-Hurek, B.; Hurek, T. *Curr. Opin. Plant Biol.* **2011**, *14*, 435.
- (15) Kunst, F.; Ogasawara, N.; Moszer, I.; Albertini, A. M.; Alloni, G.; Azevedo, V.; Bertero, M. G.; Bessieres, P.; Bolotin, A.; Borchert, S.; Borriss, R.; Boursier, L.; Brans, A.; Braun, M.; Brignell, S. C.; Bron, S.; Brouillet, S.; Bruschi, C. V.; Caldwell, B.; Capuano, V.; Carter, N. M.; Choi, S. K.; Codani, J. J.; Connerton, I. F.; Danchin, A.; et al. *Nature* **1997**, *390*, 249.
- (16) Oh, D. C.; Jensen, P. R.; Kauffman, C. A.; Fenical, W. *Bioorg. Med. Chem.* **2005**, *13*, 5267.
- (17) Oh, D. C.; Kauffman, C. A.; Jensen, P. R.; Fenical, W. *J. Nat. Prod.* **2007**, *70*, 515.
- (18) Scherlach, K.; Hertweck, C. *Org. Biomol. Chem.* **2009**, *7*, 1753.
- (19) Schroeckh, V.; Scherlach, K.; Nutzm ann, H. W.; Shelest, E.; Schmidt-Heck, W.; Schuemann, J.; Martin, K.; Hertweck, C.; Brakhage, A. A. *Proc. Natl. Acad. Sci. USA* **2009**, *106*, 14558.
- (20) Yang, J. Y.; Sanchez, L. M.; Rath, C. M.; Liu, X.; Boudreau, P. D.; Bruns, N.; Glukhov, E.; Wodtke, A.; de Felicio, R.; Fenner, A.; Wong, W. R.; Lington, R. G.; Zhang, L.; Debonsi, H. M.; Gerwick, W. H.; Dorrestein, P. C. *J. Nat. Prod.* **2013**, *76*, 1686.

(21) Watrous, J.; Roach, P.; Alexandrov, T.; Heath, B. S.; Yang, J. Y.; Kersten, R. D.; van der Voort, M.; Pogliano, K.; Gross, H.; Raaijmakers, J. M.; Moore, B. S.; Laskin, J.; Bandeira, N.; Dorrestein, P. C. *Proc. Natl. Acad. Sci. U S A* **2012**, *109*, E1743.

(22) Nguyen, D. D.; Wu, C. H.; Moree, W. J.; Lamsa, A.; Medema, M. H.; Zhao, X.; Gavilan, R. G.; Aparicio, M.; Atencio, L.; Jackson, C.; Ballesteros, J.; Sanchez, J.; Watrous, J. D.; Phelan, V. V.; van de Wiel, C.; Kersten, R. D.; Mehnaz, S.; De Mot, R.; Shank, E. A.; Charusanti, P.; Nagarajan, H.; Duggan, B. M.; Moore, B. S.; Bandeira, N.; Palsson, B. O.; Pogliano, K.; Gutierrez, M.; Dorrestein, P. C. *Proc. Natl. Acad. Sci. U S A* **2013**, *110*, E2611.

(23) Liaw, C. C.; Chen, P. C.; Shih, C. J.; Tseng, S. P.; Lai, Y. M.; Hsu, C. H.; Dorrestein, P. C.; Yang, Y. L. *Sci. Rep.* **2015**, *5*, 12856.

(24) Kleigrewe, K.; Almaliti, J.; Tian, I. Y.; Kinnel, R. B.; Korobeynikov, A.; Monroe, E. A.; Duggan, B. M.; Di Marzo, V.; Sherman, D. H.; Dorrestein, P. C.; Gerwick, L.; Gerwick, W. H. *J. Nat. Prod.* **2015**, *78*, 1671.

(25) Duncan, K. R.; Crusemann, M.; Lechner, A.; Sarkar, A.; Li, J.; Ziemert, N.; Wang, M.; Bandeira, N.; Moore, B. S.; Dorrestein, P. C.; Jensen, P. R. *Chem. Biol.* **2015**, *22*, 460.

(26) Briand, E.; Bormans, M.; Gugger, M.; Dorrestein, P. C.; Gerwick, W. H. *Environ. Microbiol.* **2016**, *18*, 384.

(27) Esquenazi, E.; Yang, Y. L.; Watrous, J.; Gerwick, W. H.; Dorrestein, P. C. *Nat. Prod. Rep.* **2009**, *26*, 1521.

(28) Debois, D.; Hamze, K.; Guerineau, V.; Le Caer, J. P.; Holland, I. B.; Lopes, P.; Ouazzani, J.; Seror, S. J.; Brunelle, A.; Laprevote, O. *Proteomics* **2008**, *8*, 3682.

- (29) Gonzalez, D. J.; Haste, N. M.; Hollands, A.; Fleming, T. C.; Hamby, M.; Pogliano, K.; Nizet, V.; Dorrestein, P. C. *Microbiol.* **2011**, *157*, 2485.
- (30) Phelan, V. V.; Liu, W. T.; Pogliano, K.; Dorrestein, P. C. *Nat. Chem. Biol.* **2012**, *8*, 26.
- (31) Moree, W. J.; Phelan, V. V.; Wu, C. H.; Bandeira, N.; Cornett, D. S.; Duggan, B. M.; Dorrestein, P. C. *Proc. Natl. Acad. Sci. U S A* **2012**, *109*, 13811.
- (32) Hoefler, B. C.; Gorzelnik, K. V.; Yang, J. Y.; Hendricks, N.; Dorrestein, P. C.; Straight, P. D. *Proc Natl Acad Sci U S A* **2012**, *109*, 13082.
- (33) Straight, P. D.; Willey, J. M.; Kolter, R. *J. Bacteriol.* **2006**, *188*, 4918.
- (34) Frey-Klett, P.; Burlinson, P.; Deveau, A.; Barret, M.; Tarkka, M.; Sarniguet, A. *Microbiol. Mol. Biol. Rev.* **2011**, *75*, 583.
- (35) Carrillo, C.; Teruel, J. A.; Aranda, F. J.; Ortiz, A. *Biochim. Biophys. Acta* **2003**, *1611*, 91.
- (36) Gonzalez, D. J.; Xu, Y.; Yang, Y. L.; Esquenazi, E.; Liu, W. T.; Edlund, A.; Duong, T.; Du, L.; Molnar, I.; Gerwick, W. H.; Jensen, P. R.; Fischbach, M.; Liaw, C. C.; Straight, P.; Nizet, V.; Dorrestein, P. C. *J. Proteomics* **2012**, *75*, 5069.
- (37) Fang, J.; Dorrestein, P. C. *Curr. Opin. Microbiol.* **2014**, *19*, 120.
- (38) Touboul, D.; Brunelle, A. *Bioanalysis* **2016**, *8*, 367.
- (39) De Pascale, G.; Wright, G. D. *ChemBiochem* **2010**, *11*, 1325.

- (40) Saunders, M.; Kohn, L. M. *Appl. Environ. Microb.* **2008**, *74*, 136.
- (41) Pedras, M. S. C.; Yaya, E. E.; Glawischnig, E. *Nat. Prod. Rep.* **2011**, *28*, 1381.
- (42) Bicas, J. L.; Dionisio, A. P.; Pastore, G. M. *Chem. Rev.* **2009**, *109*, 4518.
- (43) Marostica, M. R.; Pastore, G. M. *Food Sci. Biotechnol.* **2009**, *18*, 833.
- (44) Zikmundova, M.; Drandarov, K.; Bigler, L.; Hesse, A.; Werner, C. *Appl. Environ. Microb.* **2002**, *68*, 4863.
- (45) Agusta, A.; Maehara, S.; Ohashi, K.; Simanjuntak, P.; Shibuya, H. *Chem. Pharm. Bull.* **2005**, *53*, 1565.
- (46) Zhang, J. Z.; Zhang, L. H.; Wang, X. H.; Qiu, D. Y.; Sun, D.; Gu, J. Q.; Fang, Q. *C. J. Nat. Prod.* **1998**, *61*, 497.
- (47) Shibuya, H.; Agusta, A.; Ohashi, K.; Maehara, S.; Simanjuntak, P. *Chem. Pharm. Bull.* **2005**, *53*, 866.
- (48) Shiono, Y.; Hatakeyama, T.; Murayama, T.; Koseki, T. *Nat. Prod. Commun.* **2012**, *7*, 1065.
- (49) Ballantine, J. A.; Ferrito, V.; Hassall, C. H.; Jones, V. I. P. *J. Chem. Soc. C* **1969**, 56.
- (50) Burghart-Stoll, H.; Bruckner, R. *Organic Lett.* **2011**, *13*, 2730.
- (51) Burghart-Stoll, H.; Brückner, R. *Eur. J. Org. Chem.* **2012**, *2012*, 3978.
- (52) van Overbeek, L. S.; Saikkonen, K. *Trends Plant Sci.*, *21*, 230.

- (53) Benoit, I.; van den Esker, M. H.; Patyshakuliyeva, A.; Mattern, D. J.; Blei, F.; Zhou, M.; Dijksterhuis, J.; Brakhage, A. A.; Kuipers, O. P.; de Vries, R. P.; Kovacs, A. T. *Environ. Microbiol.* **2015**, *17*, 2099.
- (54) Scherlach, K.; Graupner, K.; Hertweck, C. *Ann. Rev. Microbiol.* **2013**, *67*, 375.
- (55) Estrada, A. E. R.; Hegeman, A.; Kistler, H. C.; May, G. *Fungal Genet. Biol.* **2011**, *48*, 874.
- (56) Jonkers, W.; Estrada, A. E.; Lee, K.; Breakspear, A.; May, G.; Kistler, H. C. *Appl Environ. Microbiol.* **2012**, *78*, 3656.
- (57) Deutsch, E. W.; Mendoza, L.; Shteynberg, D.; Farrah, T.; Lam, H.; Tasman, N.; Sun, Z.; Nilsson, E.; Pratt, B.; Prazen, B.; Eng, J. K.; Martin, D. B.; Nesvizhskii, A. I.; Aebersold, R. *Proteomics* **2010**, *10*, 1150.
- (58) Frank, A. M.; Bandeira, N.; Shen, Z.; Tanner, S.; Briggs, S. P.; Smith, R. D.; Pevzner, P. A. *J. Proteome Res.* **2008**, *7*, 113.
- (59) Guthals, A.; Watrous, J. D.; Dorrestein, P. C.; Bandeira, N. *Mol. BioSyst.* **2012**, *8*, 2535.
- (60) <https://gnps.ucsd.edu/ProteoSAFe/static/gnps-splash.jsp>.
- (61) Cline, M. S.; Smoot, M.; Cerami, E.; Kuchinsky, A.; Landys, N.; Workman, C.; Christmas, R.; Avila-Campilo, I.; Creech, M.; Gross, B.; Hanspers, K.; Isserlin, R.; Kelley, R.; Killcoyne, S.; Lotia, S.; Maere, S.; Morris, J.; Ono, K.; Pavlovic, V.; Pico, A. R.; Vailaya, A.; Wang, P. L.; Adler, A.; Conklin, B. R.; Hood, L.; Kuiper, M.; Sander, C.; Schmulevich, I.; Schwikowski, B.; Warner, G. J.; Ideker, T.; Bader, G. D. *Nat. Protoc.* **2007**, *2*, 2366.

(62) Deininger, S. O.; Cornett, D. S.; Paape, R.; Becker, M.; Pineau, C.; Rauser, S.; Walch, A.; Wolski, E. *Anal. Bioanal. Chem.* **2011**, *401*, 167.

(63) Brunelle, A.; Touboul, D.; Laprevote, O. *J. Mass Spectrom.* **2005**, *40*, 985.